Fibers and Polymers 2021, Vol.22, No.2, 314-322
DOI 10.1007/s12221-021-0121-z

ISSN 1229-9197 (print version)
ISSN 1875-0052 (electronic version)

Analysis of PLA Blends Using Weighted Relaxation Spectrum

Hyunkyu Jang[1], Junghaeng Lee[1], Mi Kyung Kwon[2], Kwan Ho Seo[1], and Kwang Soo Cho[1]*

[1]*Department of Polymer Science and Engineering, Kyungpook National University, Daegu 41566, Korea*
[2]*Division of Biotechnology, Daegu Gyeongbuk Institute of Science and Technology (DGIST), Daegu 42988, Korea*
(Received February 4, 2020; Revised May 8, 2020; Accepted May 24, 2020)

Abstract: This paper suggests a viscoelastic method to analyze microscopic structure of polymer blends which could be characterized by DMA and TEM. The viscoelastic method is to use weighted relaxation spectrum. We used poly(lactic acid)/ poly(butylene adipate-co-terephthalate) and poly(lactic acid)/poly(vinyl acetate) blends in order to check the validity of the viscoelastic method. The former is an immiscible blend and the latter is a miscible blend.

Keywords: Poly(lactic acid), Poly(butylene adipate-co-terephthalate), Poly(vinyl acetate), Weighted relaxation spectrum, Microstructure

Introduction

It has been a continuous issue how to reduce the waste from petroleum-based polymers. Biodegradable polymer may be one of the solutions of the environmental problem. Poly(lactic acid) (PLA) is one of the most promising polymers among biodegradable ones because it can be produced in large scale from regenerable sources such as corn or sugar beets [1]. Since PLA is a thermoplastic polymer, it can be shaped by melt spinning, injection molding and sheet extrusion [2]. However, PLA has demerits in impact strength, heat resistance, gas barrier property and so on [3,4]. Hence, there have been various attempts to improve the demerits of PLA through chemical modification, blending with other polymers, and nanocomposite [5-7].

One of the most important improvements is to blend PLA with a rubbery material such as poly(butylene adipate-co-terephthalate) (PBAT). However, since PBAT and PLA are not miscible, the improvement of impact strength is limited [9,10]. Further improvement of impact strength would be done by modification of the interface between PLA and PBAT, which is a popularly used modification in rubber toughening [11]. Hence, it is necessary to investigate the miscibility of various polymers with PLA. It is well-known that a miscibility test is conducted by DSC or DMA [12].

If two polymers are miscible then the blend has a single glass transition temperature. Since rubbery polymer usually has low glass transition temperature, high miscibility deteriorates the heat resistance of the PLA blends. Hence, it is necessary to find an immiscible PLA blend which has enhanced interface. This means that we have to develop an analytical method to characterize the enhancement of the interface of PLA blends.

Viscoelastic method is known as one of the simplest methods to investigate the interfacial relaxation of immiscible polymer blends [13-17]. It is also known that relaxation spectrum is the best in distinguishing structural difference among various viscoelastic functions [18]. Shaayegan *et al*. [15], Nofar *et al*. [16] and Kwon and Cho [17] used weighted relaxation spectrum, which is the product of relaxation time and relaxation spectrum, because it provides interfacial relaxation as a peak. However, these researchers did not investigate how the interfacial peak changes as the composition of binary blends.

In this paper, we will apply the methodology of Kwon and Cho [17] to PLA/PBAT blends as an immiscible pair and PLA/PVAc blends as a miscible blend. Here, PVAc is the abbreviation of poly(vinyl acetate). We check the validity of our expectation about the ability of weighted relaxation spectrum by use of DMA (dynamic mechanical analyzer) and TEM (transmission electron microscopy). It can be said that the height and position of the interfacial peak can quantify the microstructure of immiscible polymer blends. Furthermore, we expect that this methodology will contribute to the development of the PLA blends with improved interfacial properties.

Relaxation Time Spectrum

According to the viscoelastic theory, the shear stress of all linear viscoelastic materials can be formulated by the Boltzmann superposition principle [19]:

$$\sigma(t) = \int_{-\infty}^{t} G(t-\tau)\frac{\mathrm{d}\gamma(\tau)}{\mathrm{d}t}\mathrm{d}\tau \quad (1)$$

where $\sigma(t)$ is shear stress, $\gamma(t)$ is shear strain, and $G(t)$ is relaxation modulus which is one of the material functions of linear viscoelastic materials. The relaxation modulus can be measured by the strain $\gamma(t) = \gamma_0\Theta(t)$, where γ_0 is the strain amplitude and $\Theta(t)$ is the unit step function which is unity whenever t is not negative and zero otherwise.

It is well-known that the relaxation modulus of a viscoelastic fluid obeys the generalized Maxwell model:

$$G(t) = \Sigma_{i=1}^{N} G_i e^{-t/\lambda_i} \quad (2)$$

where G_i implies the relaxation intensity of the relaxation

*Corresponding author: polphy@knu.ac.kr

mode with the relaxation time λ_i. The set of relaxation intensities and relaxation times $\{G_i, \lambda_i; N\}$ is usually called discrete relaxation spectrum. However, the discrete relaxation spectrum cannot be determined uniquely from a given set of experimental data [20]. Hence, discrete relaxation spectrum is an approximation of material function rather than a genuine material function.

On the other hand, the continuous version of the generalized Maxwell model provides a genuine material function called continuous relaxation spectrum, simply relaxation spectrum:

$$G(t) = \int_{-\infty}^{\infty} H(\lambda) e^{-t/\lambda} d\log\lambda \tag{3}$$

where, $H(\lambda)$ is the continuous relaxation spectrum which is the generalization of the correspondence between G_i and λ_i. Thanks to the uniqueness of the Laplace transform and the Fourier transform, it is known that the unique $H(\lambda)$ exists for a given $G(t)$ [18]. In other words, relaxation spectrum $H(\lambda)$ is also a material function equivalent to relaxation modulus $G(t)$. However, $H(\lambda)$ cannot be measured directly by any experimental methods but can be calculated from $G(t)$ which can be measured. Nevertheless, $H(\lambda)$ is wanted to be determined because it has higher resolution than any other linear viscoelastic function [18]. Here, high resolution implies that $H(\lambda)$ can distinguish different materials more accurately than any other linear viscoelastic functions. Furthermore, if $H(\lambda)$ is known then other linear viscoelastic functions can be determined. One of the examples is

$$G'(\omega) = \int_{-\infty}^{\infty} H(\lambda) \frac{\lambda^2\omega^2}{1+\lambda^2\omega^2} d\log\lambda;$$
$$G''(\omega) = \int_{-\infty}^{\infty} H(\lambda) \frac{\lambda\omega}{1+\lambda^2\omega^2} d\log\lambda \tag{4}$$

where $G'(\omega)$ is storage modulus, $G''(\omega)$ is loss modulus, and ω is angular frequency.

There have been developed a number of algorithms which can determine relaxation spectrum with minimizing the effect of measurement errors in measurable viscoelastic functions such as dynamic and relaxation moduli [21-26]. Among them, we choose the fixed-point iteration [23] because it is one of the simplest algorithms. This algorithm was also used by Kwon and Cho [17].

For the linear viscoelasticity of multi-component system, the weighted relaxation spectrum $\lambda H(\lambda)$ gives better understanding than $H(\lambda)$ because the weighted relaxation spectrum shows peak-like appearance. The use of weighted relaxation spectrum is frequently found in literatures [15-17]. Note that if $H(\lambda)$ is given then the determination of $\lambda H(\lambda)$ is straightforward.

The Gramespacher-Meissner Model

As aforementioned, many peaks in $\lambda H(\lambda)$ could be assigned to the ingredients of a muti-component viscoelastic material. The peak-assignment in immiscible polymer blends can be validated by the Gramespacher-Meissner model [13]:

$$G^*(\omega) = \phi G^*_{\text{dis}}(\omega) + (1-\phi) G^*_{\text{mat}}(\omega) + G^*_{\text{int}}(\omega) \tag{5}$$

where $G^*(\omega) = G'(\omega) + iG''(\omega)$ is the complex modulus of the immiscible polymer blend, ϕ is the volume fraction of the dispersed phase, and the subscript dis, mat and int mean dispersed phase, matrix phase, and interface, respectively. Gramespacher and Meissener showed that equation (5) agrees very well with experimental data. Equation (5) immediately results in

$$H(\lambda) = \phi H_{\text{dis}}(\lambda) + (1-\phi) H_{\text{mat}}(\lambda) + H_{\text{int}}(\lambda) \tag{6}$$

Of course, this decomposition holds for the weighted relaxation spectrum. Equation (6) allows us to recognize the interfacial relaxation (H_{int}) from the knowledge of H_{dis} and H_{mat} which can be determined from the pure ingredients.

The Gramespacher-Meissner model was not derived from rigorous mathematics and mechanics but was the consequence from an intuitive speculation. On the other hand, Palierne [27] derived his model on the rigorous foundation of mathematics and mechanics. However, the Palierne model is expressed in a very complicated form. Kwon and Cho [17] showed that the Palierne model is almost the same with the Gramespacher-Meissner model in calculated results. Hence, it can be said that the decomposition of Equation (6) has a firm foundation.

Experimental

Materials

PLA (Ingeo™ Biopolymer 4032D), PBAT (S-Enpol PBG7070), and PVAc (no. 387924) were purchased from NatureWorks, Lotte Fine Chemical, and Sigma Aldrich, respectively. Mixtures of them were prepared by an internal mixer (Brabender® W50 EHT) with the addition of antioxidants (Total 0.1 phr; SONGNOX1010 0.05 phr and SONGNOX1680 0.05 phr). The mixing conditions were as follows: mixing time of 15 minutes, mixing speed of 50 rpm, and temperature of 175 °C. All component polymers were dried at 80 °C for 15 hours in vacuum oven before mixing.

The sample code PVAcX is the blends of PVAc and PLA with X percent as the weight fraction of PVAc. Hence, PVAc30 contains 30 wt% of PVAc. The sample code PBAT70 means the blend of PBAT (70 wt%) and PLA (30 wt%). The sample code without the number of wt% means a pure ingredient.

Dynamic Mechanical Analysis

The miscibility was investigated by the measurement of glass transition temperature using dynamic mechanical

analyzer (Perkin Elmer DMA 8000). The test specimen was prepared by a hot press with the size of 0.5 mm×10 mm×50 mm. The test conditions were as follows: frequency of 1 Hz, heating rate of 5 °C/min, and displacement amplitude of 0.001 mm. We adopted the ranges of temperature: -40-80 °C for PLA/PBAT mixtures and 0-80 °C for PLA/PVAc mixtures. The deformation mode was tensile mode.

Morphology

The morphology of dispersed phase was observed by TEM (Hitach HT7700) without staining. The samples were obtained by cryo-microtome and the acceleration voltage of TEM was 100 kV.

Rheological Measurement

We used AR-2000Ex (TA) for the linear viscoelasticity in molten state. Dynamic test mode was adopted using parallel-plate fixture. The measurement was done under nitrogen gas at 175 °C. We checked a linear regime and fixed the stress amplitude as 250 Pa.

Results and Discussion

Dynamic Mechanical Analysis

Figure 1 is the collection of the results from dynamic mechanical analysis (DMA). Figures 1(a) and 1(c) are the raw data of DMA: dynamic Young's modulus and loss tangent as functions of temperature. The peak positions of loss tangent are considered as glass transition temperature. Since the glass transition temperatures of PLA, PBAT, and PVAc are 60.1 °C, -26.3 °C and 43.9 °C, respectively, it can be recognized that PLA/PBAT blends have two peaks around the glass transition temperatures of their pure ingredients while PLA/PVAc blends have a single peak whose position approximately obeys the Fox equation:

$$\frac{1}{T_g} = \frac{\phi}{T_1} + \frac{1-\phi}{T_2} \tag{7}$$

where T_g is the glass transition temperature of the blend when the volume fraction of the ingredient 1 is ϕ and T_1 and T_2 are the glass transition temperatures of the ingredient 1 and 2, respectively. Equation (7) is a harmonic average.

Since the three component polymers are assumed to have similar density in molten state, we can replace the volume fraction with weight fraction (equation (7)). The Fox equation holds if the two ingredients are miscible. Otherwise, the blend should have two glass transition temperatures corresponding to those of the ingredients. As seen in Figures 1(b) and 1(d), it can be said that PLA and PBAT are immiscible while PLA and PVAc are miscible. The same

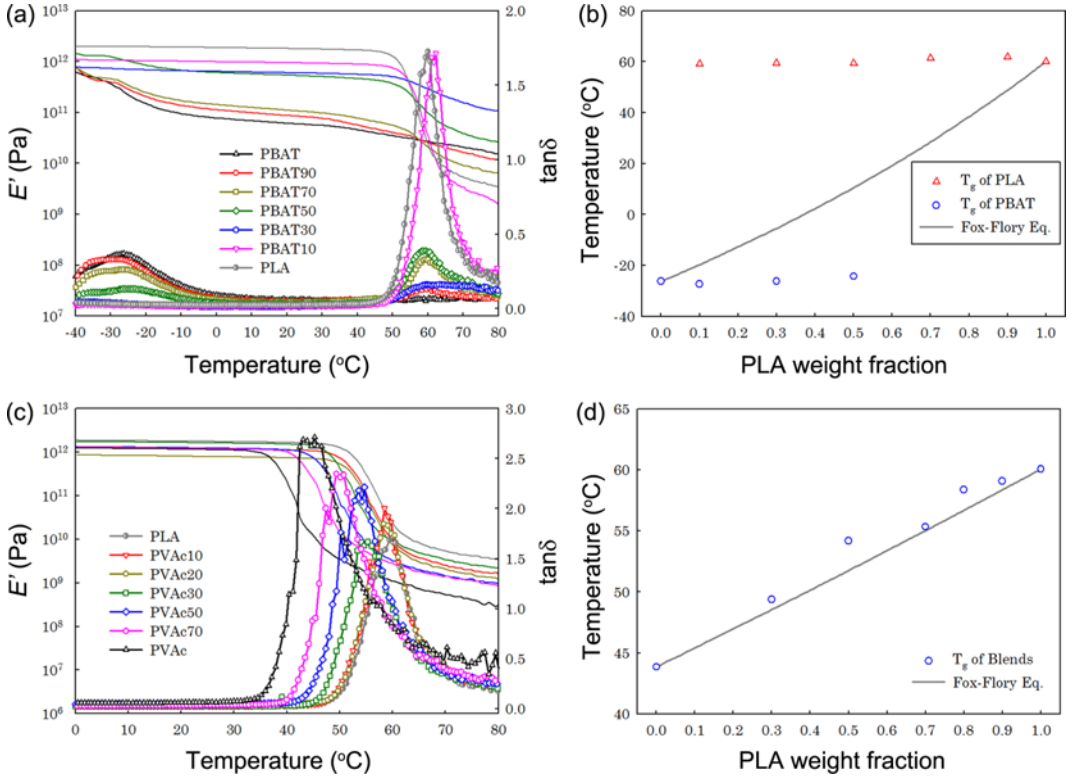

Figure 1. (a) Storage Young's modulus (E') and loss tangent tanδ as functions of temperature and (b) glass transition temperature T_g as a function of PLA weight fraction for PLA/PBAT blends. Solid lines denote E' and solid lines with symbol denote tanδ in (a), (c) and (d) are same for PLA/PVAc blends. The lines in (b) and (d) represent the Fox equation.

results have been reported in [28] and [29]. From these results, we can expect that TEM pictures of PLA/PBAT blends will show phase separation clearly and those of PLA/PVAc blends will not. For accurate analysis, thermal analysis of the polymer blends should be accompanied by discussion of crystallinity. A number of researchers have studied the effect of crystallinity of blends of PLA/PBAT [7-10] and PLA/PVAc [28,29] by use of DSC and XRD. Such studies are important for the viscoelasticity of solid polymers. However, since we focus on linear viscoelasticity of molten blends in this study, we omit such characterizations. Note that we used DMA data for checking miscibility of the blends comparing with the Fox rule.

Morphology

Since Urquijo *et al*. [30] showed that PLA/PBAT blends have sufficient contrast in transmission electron microscopy without staining, we take TEM photos without staining. PBAT-rich phase appears darker than PLA-rich phase in TEM. We found that PBAT/PVAc blends, which are not interested in this paper, also have sufficient contrast without staining. In this case, PBAT-rich phase also appears darker than PVAc-rich phase. However, we did not confirm any contrast difference between PLA and PVAc. Hence, it is hard to investigate the morphology of PLA/PVAc blends without staining. Unfortunately, we do not know how to stain the PLA/PVAc blends. Hence, we could not obtain meaningful TEM photos for PLA/PVAc blends. Since DMA data show that PLA and PVAc are miscible, we expect that the TEM photos of PLA/PVAc blends will not show any phase morphology.

Figure 2 shows the discontinuous phase structures of PLA/PBAT blends because PBAT is minor ingredient for PBAT10, PBAT20 and PBAT30 and PLA is minor ingredient for PBAT70, PBAT80 and PBAT90. As expected, the dispersed phases in PLA-rich blends look dark (PBAT10, PBAT20 and PBAT30) while the dispersed phases in PBAT-rich blends look bright (PBAT70, PBAT80 and PBAT90). Both PLA-rich and PBAT-rich blends share the same tendency that the size of them also increases as the amount of the dispersed component increases.

If the contents of the two ingredients are comparable then it is expected that the morphology would be co-continuous. We confirmed this expectation in Figure 3. PBAT35, PBAT50 and PBAT60 show co-continuous structures clearly while PBAT 65 does not. It is interesting that PBAT65 did not show the co-continuous structure although PBAT35 and PBAT65 have the same weight fraction of minor component. Since it is hard to expect a big difference in the densities of PLA and PBAT, we guess that the weight fractions of the blends are not quite different from the volume fractions. Then the structural difference between PBAT35 and PBAT65 is thought to be originated from a thermodynamic asymmetry.

The last photo of Figure 3 is that of PVAc50 which does not show any phase separation. This homogeneity could be explained by the little difference in the contrasts of PLA and PVAc. However, since DMA data mean the miscibility of the two polymers, we think that the TEM photos of PLA/PVAc blends will show such homogeneity even if staining is introduced.

The TEM observation implies that viscoelastic behavior of PLA/PBAT can be classified according to the contents of PLA: (1) PLA-dispersed structure; (2) co-continuous structure; (3) PBAT-dispersed structure. In the regimes (1) and (3), as the amount of the dispersed phase increases, we guess that the increase of interfacial area makes the increase

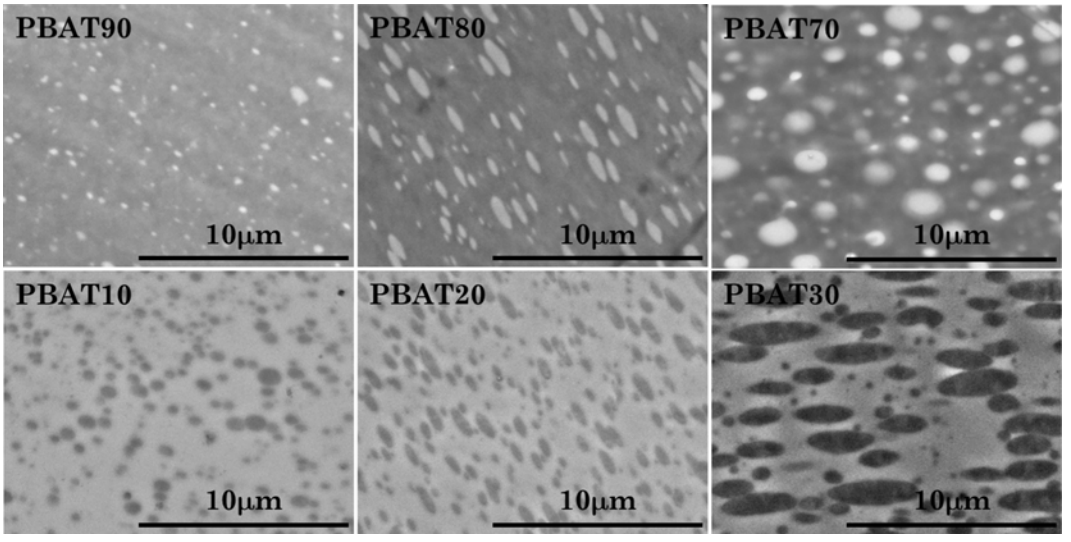

Figure 2. TEM images of PLA/PBAT blends which have discontinuous structure (PBAT90, PBAT80, PBAT70, PBAT30, PBAT20, PBAT10).

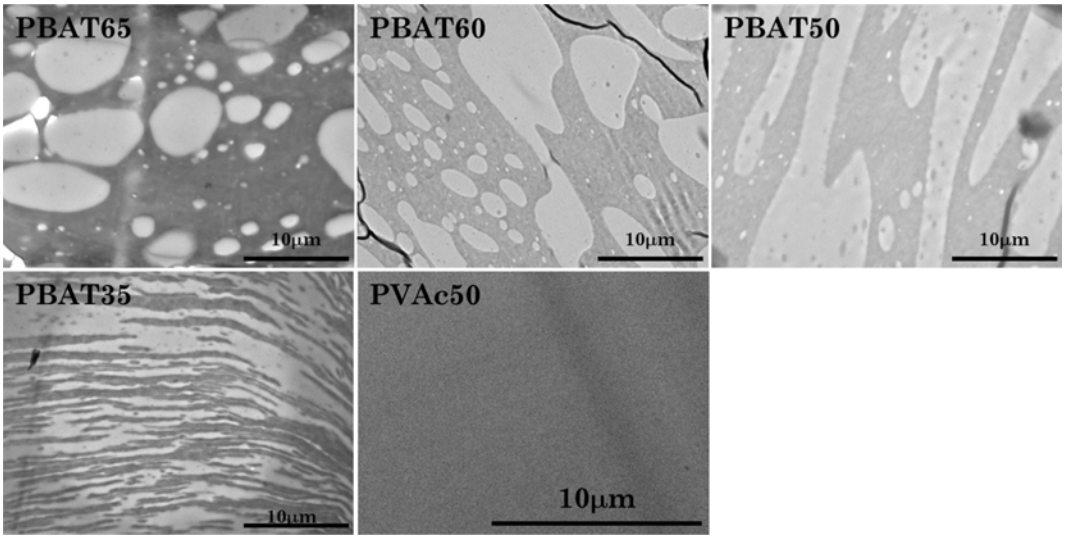

Figure 3. TEM images of PLA/PBAT blends which have co-continuous structure (PBAT65, PBAT60, PBAT50, PBAT35) and PLA/PVAc blends (PVAc50).

of a viscoelastic property. On the other hand, the viscoelastic behaviors of the regime (2) should be much different from those of the regimes (1) and (3). This expectation will be confirmed in the discussion of viscoelastic properties.

Viscoelastic Properties

Figure 4 shows the dynamic moduli of PLA/PBAT blends and PLA/PVAc blends. The dynamic moduli of PLA/PBAT blends show those of typical immiscible blends (Figures 4(a)

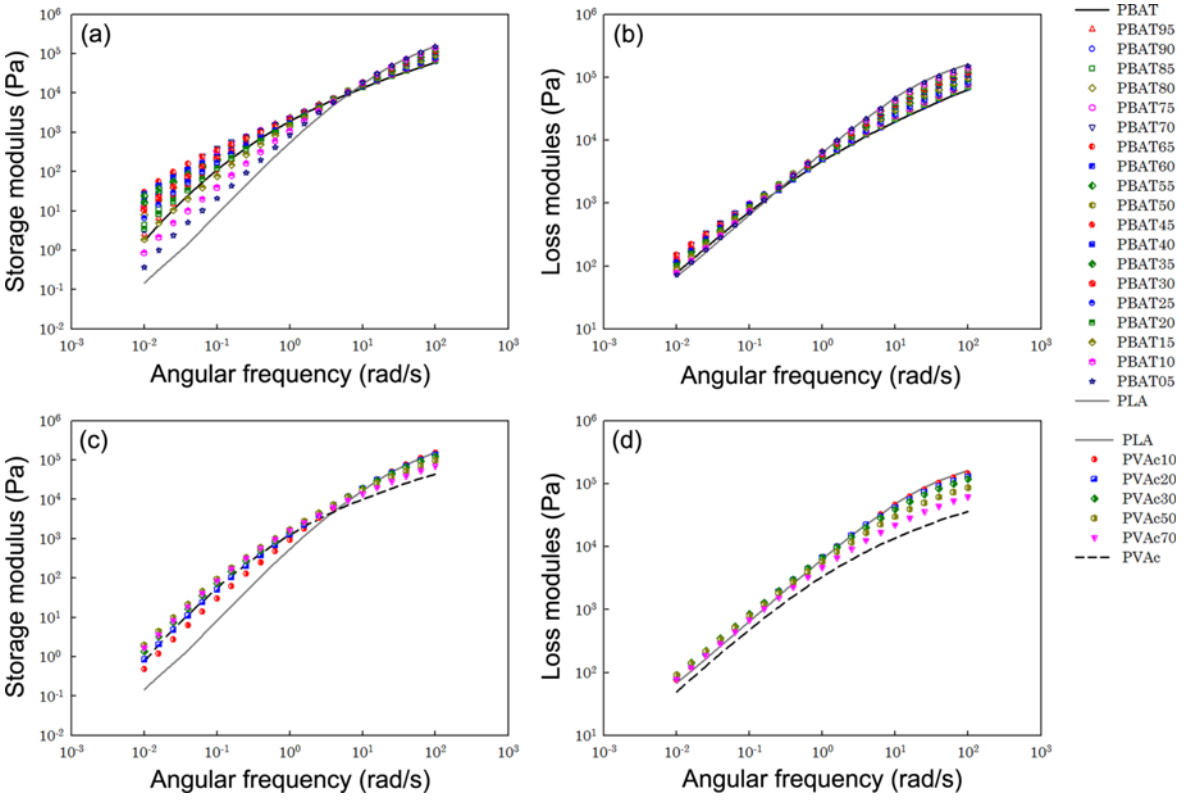

Figure 4. Dynamic moduli of experimental data to PLA/PBAT blends ((a) and (b)) and PLA/PVAc blends ((c) and (d)). Lines denote pure ingredients and symbols denote the blends.

and 4(b)). The effect of PLA contents appears bigger in storage modulus at low frequencies than in loss modulus because the deformation of interface mainly contributes to elastic behavior rather than viscous behavior. Consider a mixture of two Newtonian fluids. Since the ingredients have no elastic origins, the appearance of non-zero storage modulus of the mixture implies the effect of interface. Choi and Schowalter [31] explained theoretically such phenomena for dispersed-structures of immiscible Newtonian mixtures and Doi and Ohta [32] did it for co-continuous structures. Of course, the Gramespacher-Meissner model [13] and the Palierne model [27] also indicate that the effect of interface appears only in storage modulus.

When frequency is higher than the cross point, where loss tangent is unity, both storage and loss moduli of PLA/PBAT data are bounded by those of the pure ingredients. This means that interfacial effect is negligible at high frequency. Hence the characteristic time of interfacial relaxation is longer than the inverse of the cross frequency.

Since PLA and PVAc are miscible, it is hard to expect any interfacial effect. Hence, Figure 4(c) shows that the variation in storage modulus is not large compared with Figure 4(a). The viscoelasticity of PLA/PVAc blends is mainly bounded by those of pure ingredients in the whole range of frequency. This is typical for miscible blends.

Since interfacial effect appears in storage modulus at low frequencies, we collected the values of the storage moduli and plotted them as functions of PLA weight fraction (Figure 5). As expected, as the amount of dispersed phase increases, the storage modulus increases while different behavior is observed in the regime of co-continuous structure. Figure 2 looks like that the interfacial area increases as the amount of dispersed phase (PLA-PBAT). However, as the dispersed phases are collapsed, it is obvious that the interfacial area decreases. Figure 5 shows this tendency clearly until PLA weight fraction is less than 0.5. It

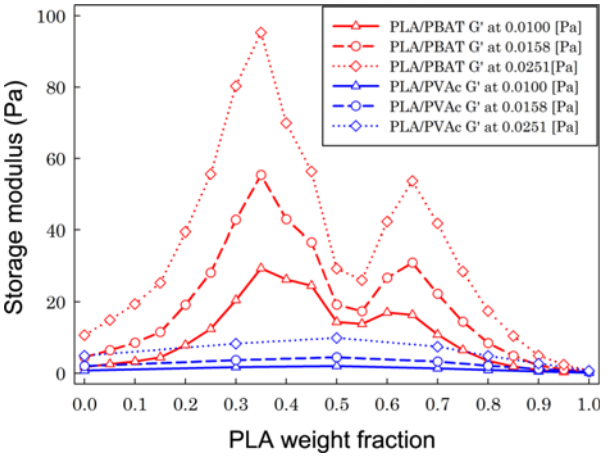

Figure 5. Comparison for storage modulus of PLA/PBAT and PLA/PVAc blends at low frequencies.

is obvious that the phase inversion occurs around the PLA weight fraction of 0.5. After the phase inversion, we can expect the interfacial area increases again until dispersed structure occurs. Hence, the variation of the storage modulus at low frequencies can be explained by use of the interfacial area. With the help of Figure 5, we can decompose the range of PLA weight fraction to four regimes: the first increase of storage modulus (PLA belongs to the dispersed phase); the first decrease of storage modulus (PBAT-rich co-continuous structure); the second increase of storage modulus (PLA-rich co-continuous structure); the second decrease of storage modulus (PBAT belongs to the dispersed phase). Different from the immiscible blend (PLA-PBAT), PLA-PVAc mixtures do not show significant variation of the storage modulus at low frequency. If any, the interfacial relaxation seems negligible in the blends of PLA and PVAc.

For more detailed analysis without relying on frequency, we need to calculate weighted relaxation spectrum [Figure 6]. The spectrum is meaningful in the interval of relaxation time which belongs to the frequency range of experiment. Because of the dimensional relation such as $\lambda \sim \omega^{-1}$, the meaningful range of relaxation time could be $\omega_{\max}^{-1} \le \lambda \le \omega_{\min}^{-1}$, where $\omega_{\min}$ and $\omega_{\max}$ are, respectively, the minimum and the maximum of the frequency range. The vertical lines in Figure 6 indicate the meaningful range of relaxation time.

Figure 6(a) shows the weighted relaxation spectra which belong to the region of the first increase of storage modulus at low frequencies. Figure 6(b) corresponds to the region of the first decrease, Figure 6(c) to the region of the second decrease and Figure 6(d) to the region of the second increase. In Figures 6(a) and 6(d), the peaks at long relaxation time represent the interfacial relaxation. We call these peaks the interfacial peaks. Compared to Figures 6(a) and 6(d), it is not easy to assign interfacial peaks in Figures 6(b) and 6(c).

As for dispersed structures, the positions and heights of interfacial peaks increases as the amount of the dispersed phases. It is a reasonable assumption that the interfacial tension does not depend on the PLA contents. The Gramespacher-Meissner model can predict the position and height of interfacial peak as functions of the composition of immiscible blend at constant interfacial tension. This was checked by Kwon and Cho [17]. The results of Figures 6(a) and 6(d) obey this tendency.

In Figures 6(b) and 6(c), only PBAT35, PBAT60 and PBAT65 show the peaks in the interval of $1\text{s} \le \lambda \le 100\text{s}$. Since the Gramespacher-Meissner model assumes that two polymers are immiscible and that the phase structure is not co-continuous, it is hard to assign interfacial peak. However, the peaks at long relaxation time obey the tendency that the peak height is proportional to the interfacial area.

Figure 7 shows the weighted relaxation spectra of PLA/PVAc blends. Since these blends are miscible, we cannot assign interfacial peak. The spectra in Figure 7 seem to be independent of PLA weight fraction. Because of the

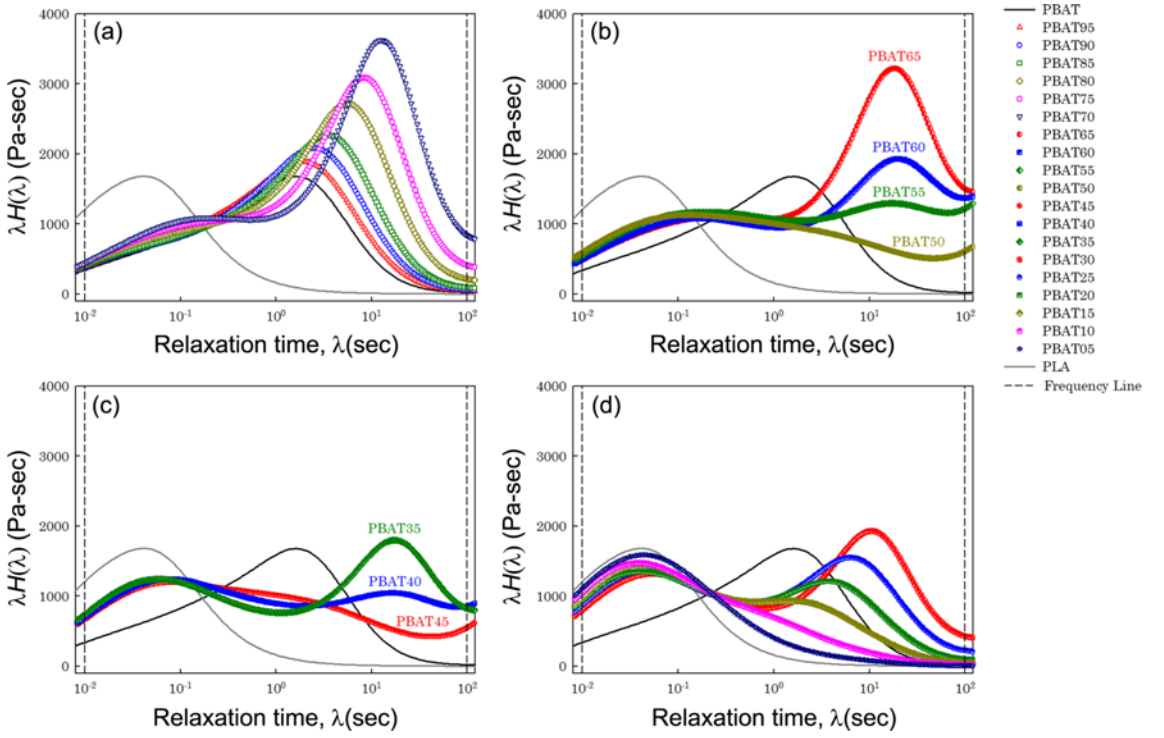

Figure 6. Weighted relaxation spectra of PLA/PBAT blends; (a) shows spectra from PBAT95 to PBAT70, (b) shows spectra from PBAT65 to PBAT50, (c) shows spectra fromPBAT45 to PBAT35, and (d) shows spectra from PBAT30 to PBAT05.

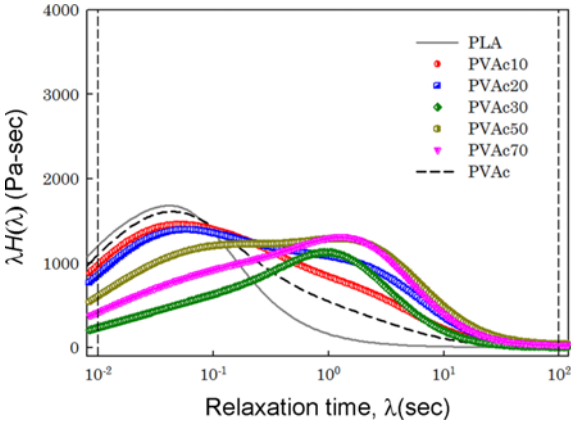

Figure 7. Weighted relaxation spectra of PLA/PVAc blends.

assumption of the Gramespacher-Meissner model, it is not meaningful to use the decomposition of equation (6). However, we tried to use the decomposition. Figure 8 shows the interfacial weighted relaxation spectra of PLA/PBAT blends (Figure 8(a)) and PLA/PVAc blends (Figure 8(b)) which were calculated from equation (6). Figure 8(b) does not show the tendency of the interfacial peaks in Figure 6, while Figure 8(a) does. This supports the miscibility of PLA and PVAc and the immiscibility of PLA and PBAT.

Figures 9 and 10 are, respectively, the position and height of the interfacial peaks of PLA/PBAT and PLA/PVAc blends

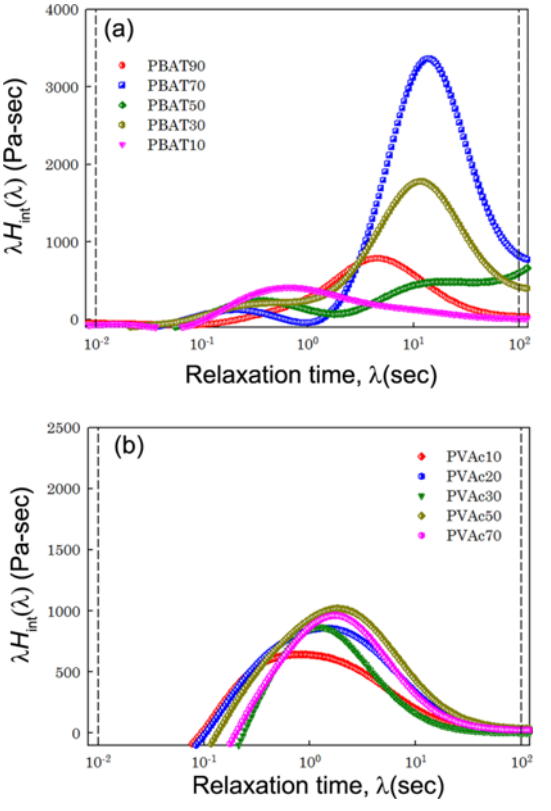

Figure 8. Interfacial weighted relaxation spectra of (a) PLA/PBAT and (b) PLA/PVAc blends.

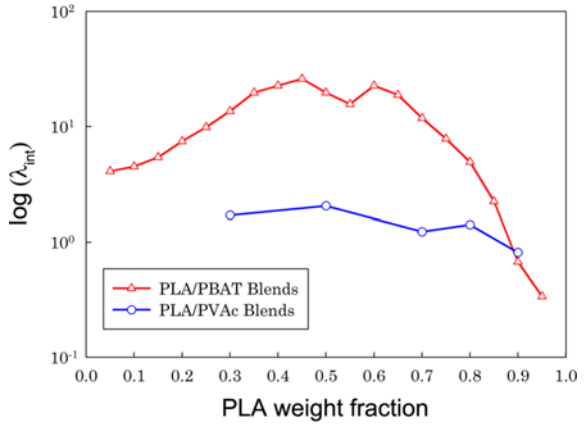

Figure 9. Peak positions (λ_{int}) of PLA/PBAT blends and PLA/PVAc blends.

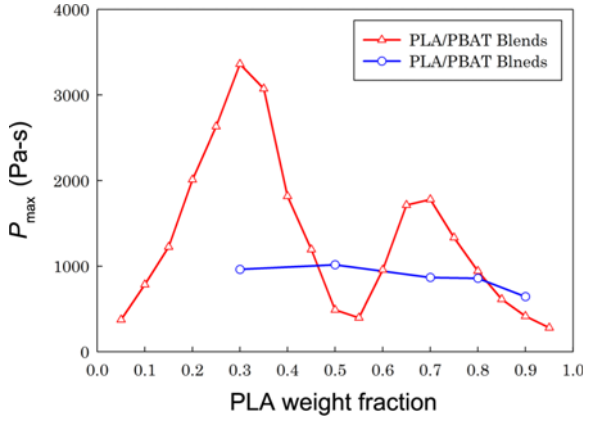

Figure 10. Peak heights (P_{max}) of PLA/PBAT and PLA/PVAc blends.

as functions of PLA contents. As for PLA/PBAT blends, the plots of both the position (λ_{int}) and height (P_{max}) of the interfacial peaks look similar to Figure 5. On the other hand, those of PLA/PVAc blends do not show such tendency. It can be said that P_{max} of PLA/PBAT blends resembles storage modulus at low frequency more than λ_{int}. One may think that Figure 10 can be replaced by Figure 5. However, Figure 5 suffers from the choice of the frequency because different materials (different PLA contents) have different material times. The frequency is just the test condition while relaxation time is a material property. Hence, Figure 5 contains the effect of test conditions while Figures 9 and 10 are independent of test conditions. Of course, Figure 5 is more practical because it does not need any data process.

We chose PLA/PBAT and PLA/PVAc blends as model systems. The results from the model systems are expected to be applied to the PLA-based systems to be developed for the enhancement of impact strength or tearing strength. It is because the enhanced PLA-based materials need an appropriate compatibilizer which can control the interface between PLA and rubbery material such as PBAT.

Conclusion

We showed that weighted relaxation spectrum can well reflect the microstructure of polymer blends because the microstructure is largely affected by the interface. We used DMA and TEM to support the validity of the application of weighted relaxation spectrum to the structure analysis. We found that the position and height of the interfacial spectrum well reflect the interfacial area. We compared immiscible blends of PLA and PBAT with miscible blends of PLA and PVAc in order to clarify that the position and height of interfacial spectrum are originated from the interface of immiscible polymers.

Acknowledgement

This research was supported by the National Research Foundation of Korea (NRF) Grant funded by the Ministry of Science and ICT for First-Mover Program for Accelerating Disruptive Technology Development (NRF-2018M3C1B9069743).

References

1. J. Pretula, S. Slomkowski, and S. Penczek, *Adv. Drug. Deliv. Rev.*, **107**, 3 (2016).
2. R. E. Drumright, P. R. Gruber, and D. E. Henton, *Adv. Mater.*, **12**, 1841 (2000).
3. S. Gu, K. Zhang, J. Ren, and H. Zhan, *Carbohydr. Polym.*, **74**, 79 (2008).
4. N. Ogata, G. Jimenez, H. Kawai, and T. Ogihara, *J. Polym. Sci. B Polym. Phys.*, **35**, 389 (1997).
5. S. S. Ray, P. Maiti, M. Okamoto, K. Yamada, and K. Ueda, *Macromoleculues*, **35**, 3104 (2002).
6. C. Nyambo, M. Misra, and A. K. Mohanty, *J. Mater. Sci.*, **47**, 5158 (2012).
7. J. Yeh, C. Tsou, C. Huang, K. Chen, C. Wu, and W. Chai, *J. Appl. Polym. Sci.*, **116**, 680 (2010).
8. Y. Deng, C. Yu, P. Wongwiwattana, and N. L. Thomas, *J. Polym. Environ.*, **26**, 3802 (2018).
9. S. Faretti, B. Cioni, and A. Lazzeri, *Macromol. Symp.*, **301**, 82 (2011).
10. L. Jiang, M. P. Wolcott, and J. Zhang, *Biomacromolecules*, **7**, 199 (2006).
11. S. Wu, *Polym. Eng. Sci.*, **30**, 753 (1990).
12. L. H. Sperling, "Introduction to Polymer Physics", 4th ed., pp.399-404, Wiley-Interscience, 2005.
13. H. Gramespacher and J. Meissner, *J. Rheol.*, **36**, 1127 (1992).
14. K. Li, J. Peng, L. Turng, and H. Huang, *Adv. Polym. Tech.*, **30**, 150 (2011).
15. V. Shaayegan, P. Wood-Adams, and N. R. Demarquette, *J.*

Rheol., **56**, 1039 (2012).
16. M. Nofar, A. Maani, H. Sojoudi, M. C. Heuzey, and P. J. Carreau, *J. Rhoel.*, **59**, 317 (2015).
17. M. K. Kwon and K. S. Cho, *Kor.-Aus. Rheol. J.*, **28**, 23 (2016).
18. K. S. Cho, M. K. Kwon, J. Lee, and S. Kim, *Kor. Aus. Rheol. J.*, **29**, 249 (2017).
19. K. S. Cho, "Viscoelasticity of Polymers", pp.287-293, Springer, 2016.
20. J.-E. Bae and K. S. Cho, *J. Non-Newtonian Fluid Mech.*, **235**, 64 (2016).
21. J. Honerkamp and J. Weese, *Rheol. Acta*, **32**, 65 (1993).
22. F. J. Stadler and C. Bailly, *Rheol. Acta*, **48**, 33 (2009).
23. K. S. Cho and G. W. Park, *J. Rheol.*, **57**, 647 (2013).
24. K. S. Cho, *J. Rheol.*, **57**, 679 (2013).
25. J.-E. Bae and K. S. Cho, *J. Rheol.*, **59**, 1081 (2015).
26. S. H. Lee, J.-E. Bae, and K. S. Cho, *Kor.-Aus. Rheol. J.*, **29**, 115 (2017).
27. J. F. Palierne, *Rheol. Acta*, **29**, 204 (1990).
28. A. M. Gajria, V. Dave, R. A. Gross, and S. P. McCarthy, *Polymer*, **37**, 437 (1996).
29. J. W. Park and S. S. Im, *Polymer*, **44**, 4341 (2003).
30. J. Urquijo, N. Aranburu, S. Dagréou, G. Guerric-Echevarría, and J. I. Eguiazábal, *Euro. Polym. J.*, **93**, 545 (2017).
31. S. J. Choi and W. R. Schowalter, *Phys. Fluids*, **18**, 420 (1975).
32. M. Doi and T. Ohta, *J. Chem. Phys.*, **95**, 1242 (1991).